A Study on Optimal Filter of Feedforward Active Noise Control System Based on Analysis of Frequency Response

Kenta Iwai and Takanobu Nishiura
College of Information Science and Engineering, Ritsumeikan University, Shiga, Japan
E-mail: {iwai18sp@fc}{nishiura@is}.ritsumei.ac.jp

***Abstract*—In this paper, we introduce an experimental study on an optimal filter of a feedforward active noise control (ANC) system based on the analysis of a frequency response. The feedforward ANC system reduces the unwanted noise by using a noise control filter based on an adaptive digital filter. The optimal noise control filter is determined by the transfer functions of each acoustic path including microphones and loudspeaker. However, this optimal filter is a noncausal filter and cannot be used in the ANC system. In this paper, the analysis of the optimal filter of the feedforward ANC system is introduced. Analytical results show that the optimal filter has a frequency characteristic similar to that of the adaptive noise control filter and the noncausal components mainly exist at low frequencies below the resonance of the secondary loudspeaker. Also, two adjustments of the optimal filter are introduced to use the optimal filter in the ANC system. Simulation results show that the adjusted filter without the noncausal component has a frequency response similar to that of the original optimal filter. Also, the simulation results show that the adjusted optimal filter can reduce the unwanted noise when using it as fixed noise control filter.**

I. Introduction

The feedforward active noise control (ANC) system is one of the solutions for noise problems [1]–[6]. ANC systems are classified into the adaptive feedforward and feedback systems [1]–[6]. In this paper, we focus on the feedforward ANC system. The structure of the basic feedforward ANC system is shown in Fig. 1. The feedforward ANC system consists of a reference microphone, an error microphone, and a secondary loudspeaker. In many cases, the feedforward ANC system uses an adaptive digital filter [7] and the filtered-x least-mean-square (FxLMS) or filtered-x normalized LMS (FxNLMS) algorithm [8], [9] is widely used as the update algorithm of the noise control filter.

In theory, the optimal filter is determined by using transfer functions of the primary, reference, and secondary paths [1], [2], [4]–[6]. In theory, this optimal filter can completely cancel the unwanted noise. However, this optimal filter cannot be used in the ANC system because it is a noncausal filter because of the nonminimum phase characteristics of each path.

In this paper, the analysis of the optimal filter of the feedforward ANC system is introduced. The analysis is conducted to compare the impulse responses and frequency characteristics of both the optimal and adaptive noise control filters. Also, two adjustments of the optimal filter are introduced to use this filter in the ANC system. The computer simulation is conducted to evaluate the noise reduction ability of the adjusted optimal filter.

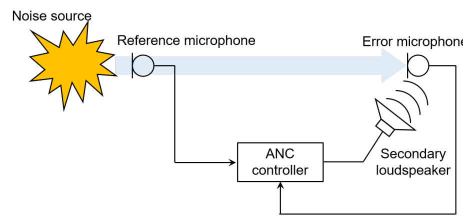

Fig. 1: Structure of basic feedforward ANC system.

II. Feedforward active noise control system and its optimal filter

A. Feedforward active noise control system

The feedforward ANC system has a noise control filter that minimizes the error signal obtained at the error microphone. The block diagram of the feedforward ANC system is shown in Fig. 2. In Fig. 2, P is the primary path between the noise source and the error microphone, R is the reference path between the noise source and the reference microphone, S is the secondary path between the secondary loudspeaker and the error microphone, W is the noise control filter, and $\hat{S}$ is the secondary path model.

The unwanted noise $v(n)$ reaches the reference microphone through the reference path. Then, the noise control filter $\mathbf{w}(n)$ is updated using the reference signal $x(n)$ picked up by the reference microphone. After updating the noise control filter $\mathbf{w}(n)$, antinoise $y'(n)$ is emitted from the secondary loudspeaker to reduce the unwanted noise $d(n)$ passing along the primary path. Here, the error signal $e(n)$ obtained at the error microphone is represented by

$$e(n) = d(n) - y_{\mathrm{S}}(n), \tag{1}$$

where n is the time index. $y_{\mathrm{S}}(n)$ is the antinoise emitted from the secondary loudspeaker and is represented as

$$y_{\mathrm{S}}(n) = \mathbf{s}^{\mathrm{T}}(n)\mathbf{y}(n), \tag{2}$$

$$y(n) = \mathbf{w}^{\mathrm{T}}(n)\mathbf{x}(n), \tag{3}$$

where $\mathbf{s}(n)$ is the impulse response of the secondary path, T is the transpose operator, $\mathbf{y}(n)$ is the antinoise vector, and

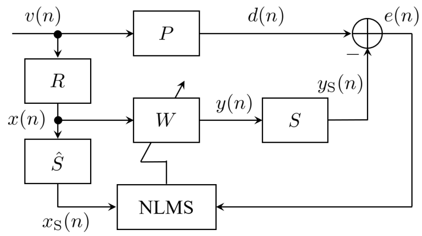

Fig. 2: Block diagram of basic feedforward ANC system.

$\mathbf{x}(n)$ is the reference signal vector. To update the noise control filter $\mathbf{w}(n)$, the FxLMS and FxNLMS algorithms [8], [9] are widely used. The update equation for the FxNLMS algorithm is represented by

$$\mathbf{w}(n+1) = \mathbf{w}(n) + \frac{\alpha e(n)\mathbf{x}_S(n)}{\|\mathbf{x}_S(n)\|^2 + \beta}, \tag{4}$$

$$x_S(n) = \hat{\mathbf{s}}^T(n)\mathbf{x}(n), \tag{5}$$

where $x_S(n)$ and $\mathbf{x}_S(n)$ are the filtered reference signal and its vector, respectively, $\|\cdot\|$ denotes the l_2 norm, α is the step size parameter $(0 < \alpha < 2)$, β is the regularization parameter with a small positive value, and $\hat{\mathbf{s}}(n)$ is the impulse response vector of the secondary path model.

B. Optimal noise control filter

The z transform of the error signal is represented as

$$E(z) = D(z) - Y_S(z), \tag{6}$$

where $E(z)$, $D(z)$, and $Y_S(z)$ are the z transforms of $e(n)$, $d(n)$, and $y_S(n)$, respectively. From (6), the optimal noise control filter $W_O(z)$ can be obtained when $E(z) = 0$ and is represented by

$$W_O(z) = \frac{P(z)}{R(z)S(z)}, \tag{7}$$

where $P(z)$, $R(z)$, and $S(z)$ are the transfer functions of the primary, reference, and secondary paths, respectively [2], [4], [5][1]. In general, the optimal filter $W_O(z)$ is a noncausal filter because the acoustic path is generally a nonminimum phase system [5]. Hence, the optimal filter cannot be used directly in the ANC system.

III. Analysis of optimal filter

In this section, the optimal filter is analyzed in the frequency domain using the frequency responses of each path and two analyses are conducted. The first analysis is a comparison of the optimal filter and each path. The second one is a comparison of the optimal filter and adaptive nose control filter. Their frequency responses were obtained from the measured impulse responses. Measurement conditions and the arrangement of the equipment are shown in Table I and Fig. 3, respectively. The identification system was implemented as shown in Fig. 4. The impulse and frequency responses of each path are shown in Figs. 5, 6, and 7, respectively. In Figs. 6 and 7, the frequency responses were obtained by 8192-point discrete Fourier transform (DFT).

[1]In general, the optimal filter depends on not only the transfer functions but also the unwanted noise [2], [4], [5], we assume that the unwanted noise is the white noise to simplify the discussion.

TABLE I: Measurement conditions for identification of impulse responses.

Input signal	White noise
Sampling frequency	8000 Hz
Frequency range	0 - 2000 Hz
Duration of input signal	30 s
Tap length of primary path P	300
Tap length of reference path R	300
Tap length of secondary path S	300
Update algorithm of adaptive filter	NLMS algorithm
Step size parameter	0.01
Regularization parameter	1.0×10^{-5}

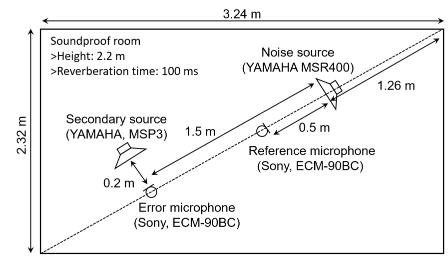

Fig. 3: Arrangement of measurement equipment.

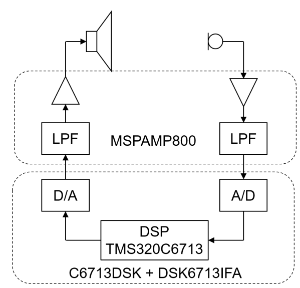

Fig. 4: Implementation of identification system.

A. Analysis 1: optimal filter and each path

The optimal filter under this condition was obtained from the frequency responses shown in Figs. 6 and 7 with 8192-point DFT, i.e.,

$$W_O(\omega) = \frac{P(\omega)}{R(\omega)S(\omega)}, \tag{8}$$

where $P(\omega)$, $R(\omega)$, and $S(\omega)$ are the frequency responses of the primary, reference, and secondary paths, respectively, and ω is the angular frequency. The impulse and frequency responses of the optimal filter are shown in Fig. 8. From Fig. 8, it can be seen that the optimal filter is a noncausal filter. Also, it can be seen that the amplitude of the frequency response is

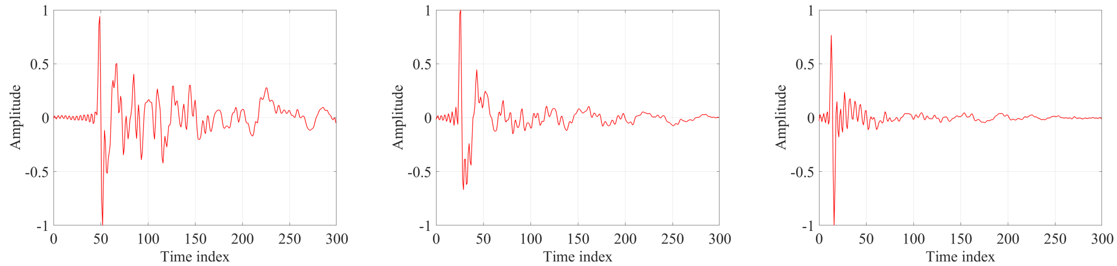

(a) Primary path (b) Reference path (c) Secondary path

Fig. 5: Impulse responses of each path.

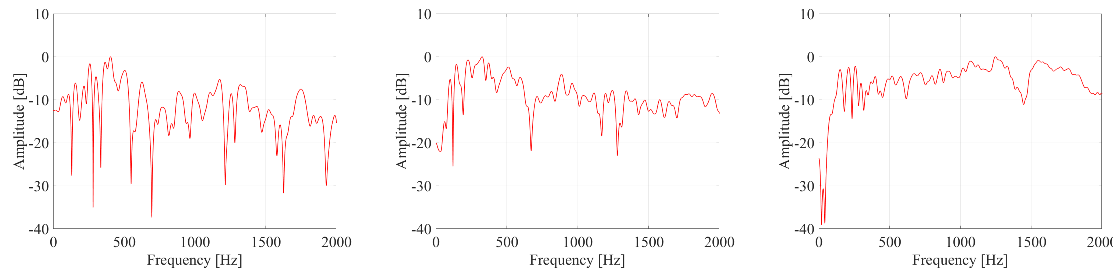

(a) Primary path (b) Reference path (c) Secondary path

Fig. 6: Frequency–amplitude characteristics of each path.

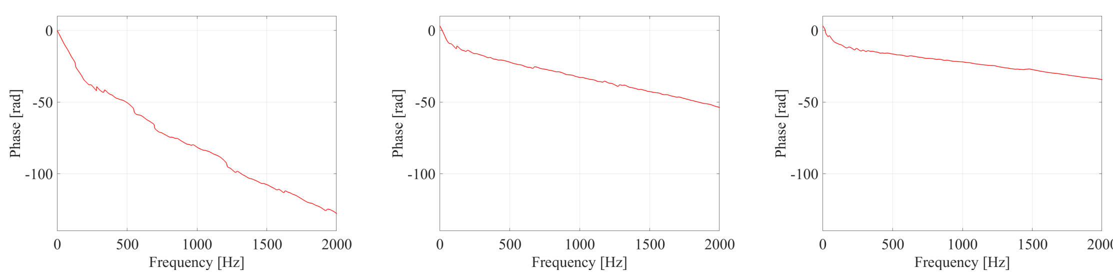

(a) Primary path (b) Reference path (c) Secondary path

Fig. 7: Frequency–phase characteristics of each path.

very large and the phase increases at low frequencies. Hence, the optimal filter cannot be used in the ANC system.

The frequency response of the optimal filter can be separated as

$$W_{\mathrm{O}}(\omega) = \frac{P(\omega)}{R(\omega)} \frac{1}{S(\omega)}. \quad (9)$$

The frequency responses $P(\omega)/R(\omega)$ and $1/S(\omega)$ are shown in Fig. 9. As seen in Fig. 9, the amplitude characteristic of the optimal filter is similar to that of $1/S(\omega)$ at low frequencies. In this analysis, the large amplitude of $1/S(\omega)$ is related to the resonance of the secondary loudspeaker, whose resonance frequency is about 100 Hz. Hence, it can be considered that the low-frequency response of the optimal filter mainly consists of the inverse of the secondary path. Also, it is difficult to use the optimal filter in the ANC system without adjusting the low-frequency response.

B. Analysis 2: optimal and adaptive filters

The noise control filter obtained using the adaptive filter is updated by the FxNLMS algorithm with the tap length of 1024, step size of 0.01, regularization parameter of 1.0×10^{-5}, and 1,416,000 updates. The characteristics of the adaptive noise control filter are shown in Fig. 10. In Fig. 10, the frequency responses of both optimal and adaptive noise control filters are found to be similar to each other above 100 Hz. This implies that the optimal noise control filter has the capability to reduce unwanted noise via the ANC system by adjusting the low-frequency characteristic.

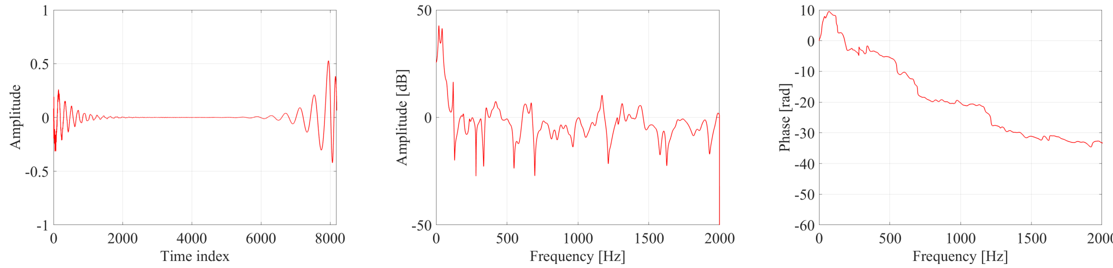

(a) Impulse response (b) Frequency–amplitude characteristic (c) Frequency–phase characteristic

Fig. 8: Characteristics of optimal filter.

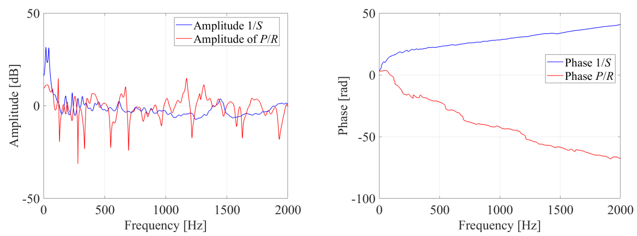

(a) Frequency–amplitude characteristic (b) Frequency–phase characteristic

Fig. 9: Characteristics of $P(\omega)/R(\omega)$ and $1/S(\omega)$.

C. Ideas for adjustment of optimal filter

From the results shown above, it can be considered that there is the capability of the ANC system using the optimal filter by adjusting the frequency response at low frequencies. Here, two adjustment methods for the optimal filter are shown [2].

The first method is to use a high-pass filter, as shown as

$$W_{\mathrm{O,A1}}(\omega) = H_{\mathrm{HPF}}(\omega) W_{\mathrm{o}}(\omega), \tag{10}$$

where $H_{\mathrm{HPF}}(\omega)$ is the frequency response of the high-pass filter. Here, the high-pass filter should have a small time delay to satisfy the causality constraint [10], [11]. By using $H_{\mathrm{HPF}}(\omega)$, the noncausal components at low frequencies are suppressed and the optimal filter becomes similar to the causal filter. The second method is to replace the frequency response of the optimal filter into $P(\omega)/R(\omega)$, as shown as

$$W_{\mathrm{O,A2}}(\omega) = 1 \begin{cases} \dfrac{P(\omega)}{R(\omega)}, & |\omega| < \omega_{\mathrm{c}}, \\ W_{\mathrm{O}}(\omega), & |\omega| \geq \omega_{\mathrm{c}}. \end{cases} \tag{11}$$

As shown in subsection III-A, the optimal filter contains both $P(\omega)/R(\omega)$ and $1/S(\omega)$ and the time delay of $P(\omega)/R(\omega)$ is smaller than that of $H_{\mathrm{HPF}}(\omega)W_{\mathrm{O}}(\omega)$. Hence, this modification can prevent the large time delay. In the following section, the noise reduction ability of each adjusted filter is shown. Also, from here after, the adjusted optimal filters $W_{\mathrm{O,A1}}(\omega)$ and $W_{\mathrm{O,A2}}(\omega)$ are denoted as adjusted optimal filter 1 and adjusted optimal filter2, respectively.

[2]In general, the adjustment of the frequency response should be conducted through some mathematical or optimization approach. However, the adjustment method shown in this paper is very simple so that the capability of the adjusted optimal filter is shown.

IV. Computer Simulation of Noise Reduction

The computer simulations were conducted to evaluate the adjusted optimal filter in terms of the frequency characteristics and noise reduction ability. In the simulations, the optimal filter was designed with 8192-point DFT. The primary, reference, and secondary paths are the same as shown in Section III. Also, the high-pass filter was designed as the second-order IIR filter with the Butterworth characteristic. The cutoff frequency was set to 100 Hz. Hereafter, the adjusted optimal filters (10) and (11) are denoted as adjusted filters 1 and 2, respectively.

The adjusted optimal filters are shown in Figs. 11 and 12, respectively. In Figs. 11 and 12, the characteristics of these adjusted optimal filters above 100 Hz are the same as that of the optimal filter without any adjustments. However, these adjusted optimal filters have small noncausal components and they should be replaced with zero. Moreover, the lengths of the causal components are too large to finish the operation in the sampling period, and they are reduced by the window function shown as

$$h_{\mathrm{Hann}} = \begin{cases} 0.5 - 0.5\cos\left(\dfrac{2\pi n}{N}\right), & N > n \geq 0, \\ 0, & n < 0, \end{cases} \tag{12}$$

where N is the tap length of the noise control filter. In the simulations, N is set to 1024. The characteristics of the adjusted filters with the window function are shown in Figs. 13 and 14. It can be seen from Figs. 13 and 14 that these characteristics are different from those of the optimal filter without any adjustments, particularly the phase characteristic. However, these adjusted filters are the causal filter and are used in the following simulation.

The adjusted optimal filters were evaluated in terms of the time waveform, the amount of noise reduction, and frequency spectra. The amount of noise reduction is defined as

$$\mathrm{Reduction}(n) = 10\log_{10}\frac{\sum_{m=0}^{N_{\mathrm{Rd}}-1} d^2(n-m)}{\sum_{m=0}^{N_{\mathrm{Rd}}-1} e^2(n-m)}, \tag{13}$$

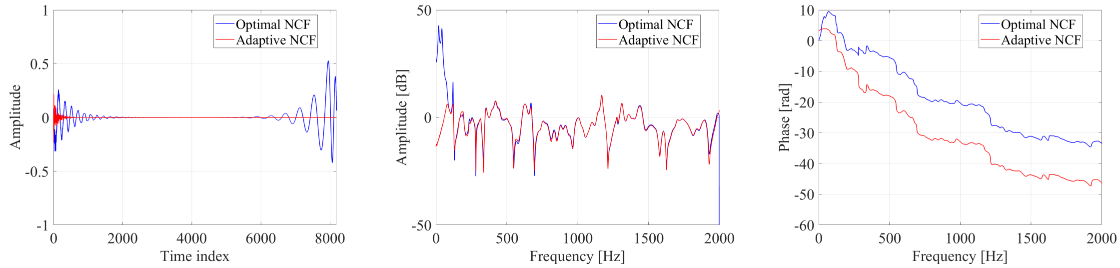

(a) Impulse response (b) Frequency–amplitude characteristic (c) Frequency–phase characteristic

Fig. 10: Characteristics of noise control filter (adaptive filter).

TABLE II: Simulation conditions.

Unwanted noise	White noise
Sampling frequency	8000 Hz
Frequency range	0 - 2000 Hz
Tap length of primary path P	300
Tap length of reference path R	300
Tap length of secondary path S	300
Tap length of secondary path model $\hat{S}$	300
Tap length of noise control filter W	1024
Update algorithm of adaptive filter	FxNLMS algorithm
Step size parameter α	0.01
Regularization parameter β	1.0×10^{-5}

where N_{Rd} is the number of samples to calculate of (13) and $\mathrm{Reduction}(n)$ was calculated for every N_{Rd} sample. The simulation conditions for the evaluation of the noise reduction ability are shown in Table II. To enable a comparison with the adaptive-filter-based ANC system shown in Fig. 2, the noise reduction ability of the basic ANC system is also evaluated. The error signals, amounts of noise reduction, and frequency spectra for each filter are shown in Figs. 15 and 16. From Figs. 15 and 16, we see that the adjusted optimal filters 1 and 2 can reduce the unwanted noise by about 6 dB and 10 dB, respectively. However, the amounts of noise reduction with both filters are smaller than that with the adaptive ANC system.

To show the reason behind these results, the frequency responses of the adjusted optimal filters and the adaptive noise control filter are shown in Figs. 17 and 18. The phase characteristics of the adjusted optimal filters are different from those of the adaptive noise control filter, although their amplitude characteristics are almost the same. In other words, it can be considered that additional adjustment for the phase characteristic should be incorporated. However, both adjusted optimal filters can reduce the unwanted noise to some extent, and thus, they can be used as fixed filters.

V. Conclusion

In this paper, the analysis of the optimal filter of the feedfoward ANC system was introduced. The analysis based on the measured frequency responses showed that the non-causal components of the optimal filter mainly exist below the resonance of the secondary loudspeaker. Also, two adjustments of the optimal filter were introduced for using this filter in the ANC system. The adjustment in the frequency domain resulted in the adjustment of the optimal filter so that this filter could be used in a ANC system. Simulation results of noise reduction showed that the adjusted filter without any noncausal component exhibits a frequency response similar to that of the original optimal filter. Also, the simulation results showed that the adjusted optimal filter can reduce the unwanted noise to some extent when using it as fixed noise control filter. In the future, the adjustment method for the phase characteristic will be developed to improve the ability of noise reduction.

Acknowledgment

A part of this work is supproted by KDDI Foundation Research Grant Program 2019 and JSPS KAKENHI (JP21K17773).

References

[1] P. Nelson and S. Elliott, *Active Control of Sound*. San Diego, CA: Academic Press, 1992.
[2] S. Elliott and P. Nelson, “Active noise control,” *IEEE Signal Process. Mag.*, vol. 10, no. 4, pp. 12–35, Oct. 1993.
[3] S. M. Kuo and D. R. Morgan, *Active Noise Control Systems: Algorithms and DSP Implementation*. New York: John Wiley & Sons, 1996.
[4] ——, “Active noise control: a tutorial review,” *Proc. IEEE*, vol. 87, no. 6, pp. 943–973, June 1999.
[5] S. Elliott, *Signal Processing for Active Control*. San Diego, CA: Academic Press, 2001.
[6] Y. Kajikawa, W. Gan, and S. Kuo, “Recent advances on active noise control: open issues and innovative applications,” *APSIPA Trans. Signal Inform. Process.*, vol. 1, pp. 1–21, Aug. 2012.
[7] S. O. Haykin, *Adaptive Filter Theory*, 4th ed. Upper Saddle River, NJ: Prentice Hall, 2001.
[8] D. Morgan, “An analysis of multiple correlation cancellation loops with a filter in the auxiliary path,” *IEEE Trans. Acoust. Speech Signal Process.*, vol. 28, no. 4, pp. 454–467, Aug. 1980.
[9] E. Bjarnason, “Analysis of the filtered-X LMS algorithm,” *IEEE Trans. Speech Audio Process.*, vol. 3, no. 6, pp. 504–514, Nov. 1995.
[10] H. Janocha and B. Liu, “Simulation approach and causality evaluation for an active noise control system,” *Proc. IEE Control Theory Appl.*, vol. 145, pp. 423–426, July 1998.
[11] X. Kong and S. Kuo, “Study of causality constraint on feedforward active noise control systems,” *IEEE Trans. Circuits Syst.*, vol. 46, no. 2, pp. 183–186, Feb. 1999.

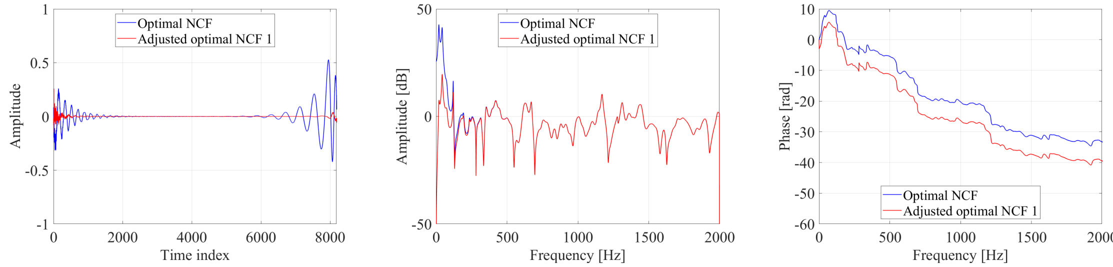

(a) Impulse response (b) Frequency–amplitude characteristic (c) Frequency–phase characteristic

Fig. 11: Characteristics of adjusted optimal filter 1.

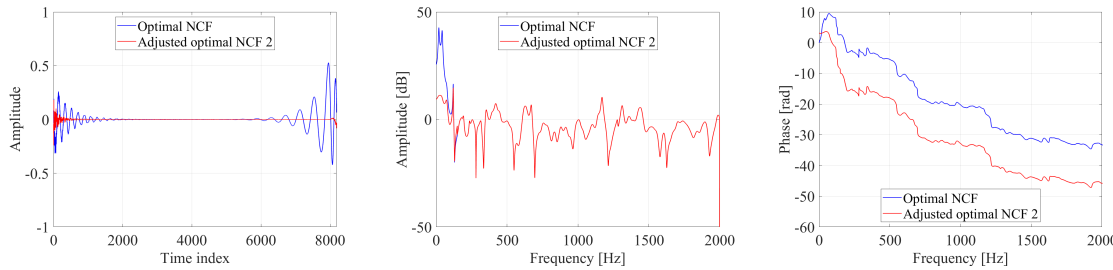

(a) Impulse response (b) Frequency–amplitude characteristic (c) Frequency–phase characteristic

Fig. 12: Characteristics of adjusted optimal filter 2.

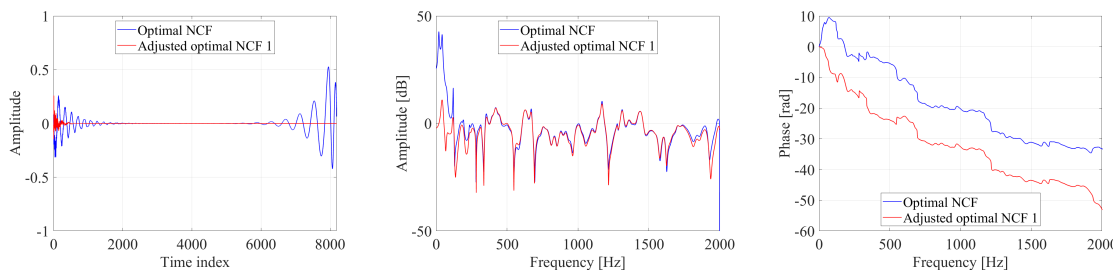

(a) Impulse response (b) Frequency–amplitude characteristic (c) Frequency–phase characteristic

Fig. 13: Characteristics of adjusted optimal filter 1 with window function.

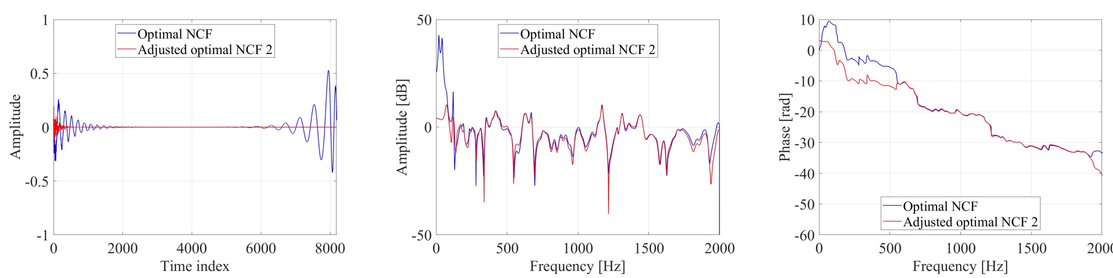

(a) Impulse response (b) Frequency–amplitude characteristic (c) Frequency–phase characteristic

Fig. 14: Characteristics of adjusted optimal filter 2 with window function.

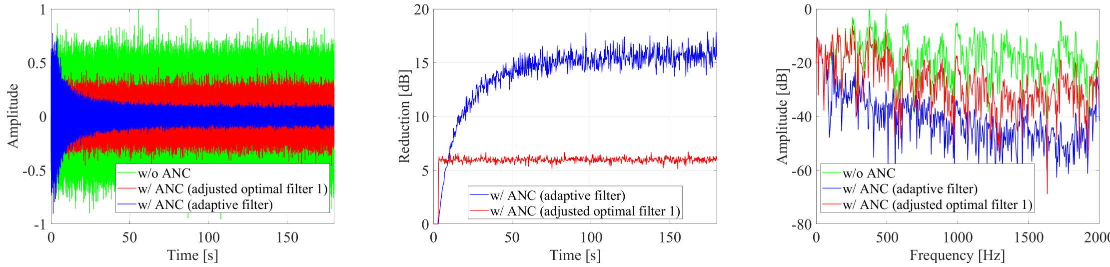

(a) Time waveform (b) Amount of noise reduction (c) Frequency spectra

Fig. 15: Amount of noise reduction (adjusted optimal filter 1).

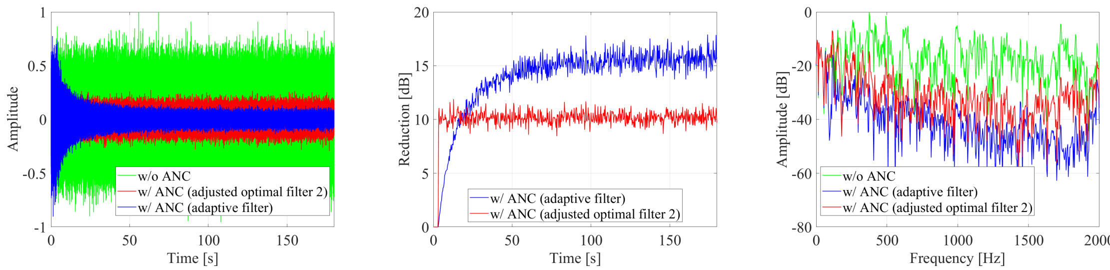

(a) Time waveform (b) Amount of noise reduction (c) Frequency spectra

Fig. 16: Amount of noise reduction (adjusted optimal filter 2).

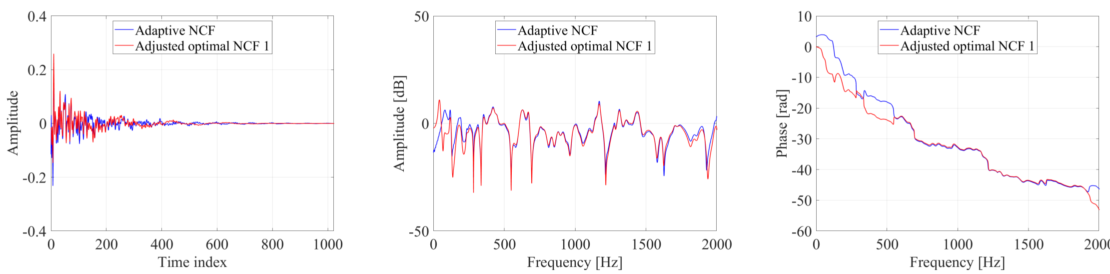

(a) Impulse response (b) Frequency–amplitude characteristic (c) Frequency–phase characteristic

Fig. 17: Results for the adjusted optimal filter 1 and adaptive noise control filter.

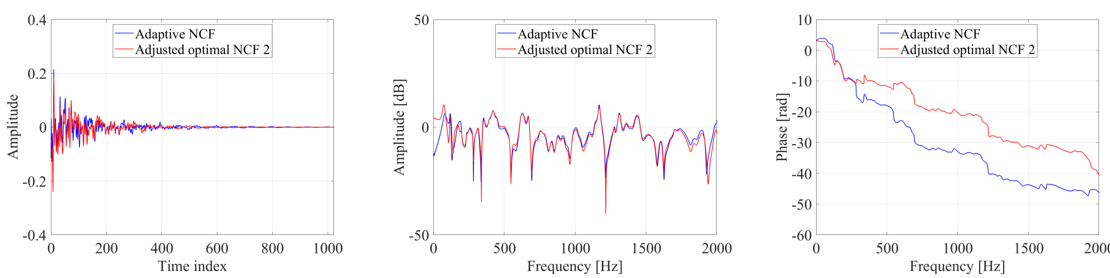

(a) Impulse response (b) Frequency–amplitude characteristic (c) Frequency–phase characteristic

Fig. 18: Results for the adjusted optimal filter 2 and adaptive noise control filter.